**Article ID:** 1007-4627(2013) 04-0503-08

# An Analytical Solution to Inhomogeneous Neutron Diffusion Equation in Accelerator Driven System

JING Tian[1], WANG Xiangqi[1], WANG Qun[2], WU Hongli[1], GONG Xiaodong[1]

( *1. National Synchrotron Radiation Laboratory, University of Science and Technology of China, Hefei 230029, China*; *2. Department of Modern Physics, University of Science and Technology of China, Hefei 230026, China* )

**Abstract:** The analytical form of the Green's functions of the inhomogeneous diffusion equation for neutrons are obtained using the Fourier method. The neutron flux distributions with the external neutron source located at arbitrary positions are calculated from the Green's functions. In a subcritical system, the dependences of the subcritical multiplication factor $k_{\rm s}$ on the source position and the core size with the fixed subcriticality $k_{\rm eff}$ are analyzed based on the series solution. It is found that $k_{\rm s}$ decreases with the core size. Although this variation is small, the energy gain is sensitive to $k_{\rm s}$ and then the core size, which has to be taken into account in the design of the source driven subcritical system.

**Key words:** ADS; neutron flux; neutron diffusion equation; subcritical multiplication factor; subcriticality

**CLC number:** TL325 **Document code:** A **DOI:** 10.11804/NuclPhysRev.30.04.503

## 1 Introduction

In recent years, the wide interest in developing the new form of Accelerator Driven System (ADS) arises to meet the urgent demand for nuclear energy and transmutation of long-life radio-toxic by-products. These by-products are generated from large number of existing nuclear power plants and raise a serious environmental problem[1−2]. Subcritical core is characterized by its intrinsic safety and ability of energy amplification[3]. Both features are due to certain degree of subcriticality of the system, conventionally described by the effective multiplication factor $k_{\rm eff}$. This factor is extracted from the eigenvalue of neutron transport equation, which obviously depends only on the inherent property of the core. However, when considering the effect of external source neutrons, we should use a new parameter subcritical multiplication factor $k_{\rm s}$ to evaluate the efficiency of external source neutrons. $k_{\rm s}$ is defined as the fraction of the fission neutrons in the subcritical system[4−6]:

$$k_{\rm s} = \frac{F}{F+S} , \tag{1}$$

$$F = \int_V \int_0^\infty {\rm d}^3\boldsymbol{r}{\rm d}E\, \nu\Sigma_{\rm f}(\boldsymbol{r},E)\phi_{\rm s}(\boldsymbol{r},E) , \tag{2}$$

$$S = \int_V \int_0^\infty {\rm d}^3\boldsymbol{r}{\rm d}E\, s(\boldsymbol{r},\ E) , \tag{3}$$

where $F$ and $S$ are total number of fission and source neutrons respectively, $V$ is the the volume of the system, $s(\boldsymbol{r},\ E)$ is the external neutron source density, $\nu$ is the average number of fission neutrons per fission reaction, $\phi_{\rm s}(\boldsymbol{r},\ E)$ is the neutron flux, and $\Sigma_{\rm f}(\boldsymbol{r},\ E)$ is the macroscopic fission cross-section.

One of main goals of ADS is to amplify the beam energy for power production. So the energy generated by total fission reactions in the multiplying medium is expected to be as high as possible for economic purpose. To evaluate the energy amplification, the energy gain $g$ is defined as the ratio of the energy produced by the secondary fissions to the proton energy[7]:

$$g = \frac{0.2k_{\rm s}N_0}{\nu(1-k_{\rm s})E_{\rm p}} , \tag{4}$$

where $N_0$ is the number of primary neutrons produced by

**Received date:** 15 Apr. 2013; **Revised date:** 4 May 2013
**Foundation item:** National Natural Science Foundation of China (11045003, 10975150)
**Biography:** JING Tian(1986–), female, Xinxiang, Henan, China, Graduate student, working on nuclear science and technology; E-mail: jingtian@mail.ustc.edu.cn.
**Corresponding author:** WANG Xiangqi, E-mail: wangxaqi@ustc.edu.cn; WANG Qun, E-mail: qunwang@ustc.edu.cn

the interaction of a proton with spallation target, $E_p$ is the proton energy. When $k_s$ approaches unity, the energy gain will be infinitely large.

To obtain a high $g$, the core should be very close to the critical point. However, a subcritical reactor operated far from the critical point is considered to be safer than the one which is nearly critical. We can see from Eq. (4) that the energy gain is directly related to the subcritical multiplication factor $k_s$, while the safety is determined by subcriticality $k_{\text{eff}}$. The two parameters are different unless the system is exactly critical. In this paper, we will build a simple subcritical reactor model with cylindrical and spherical symmetry. The model is based on diffusion approximation and captures main features of subcritical reactor. The neutron flux distribution can be obtained using the Green's function technique. An analytical expression for the multiplication factor $k_s$ can be obtained as a function of the external neutron source position and the radius of the subcritical reactor. We will investigate the difference between $k_s$ and $k_{\text{eff}}$ which may provide some guidance for the design of ADS.

## 2 Green's function for neutron diffusion equation

We consider a bare subcritical reactor model with only one energy group. The neutron flux is a function of $\boldsymbol{r}$ only. With general notations, the static neutron diffusion equation with an external source can be written as:

$$D\nabla^2\phi_s(\boldsymbol{r}) + (\nu\Sigma_f - \Sigma_a)\phi_s(\boldsymbol{r}) + s(\boldsymbol{r}) = 0\ , \tag{5}$$

$$\phi_s(\boldsymbol{r} = \text{boundary surface}) = 0\ . \tag{6}$$

Eq. (6) is the usual boundary condition in diffusion theory. Here $\Sigma_a$ is the macroscopic absorption cross section, $D$ is the diffusion constant, and the subscript 's' represents that the system is subcritical. With the material buckling $B_m$ and the source term $q(\boldsymbol{r})$,

$$B_m^2 = \frac{(\nu\Sigma_f - \Sigma_a)}{D}\ , \tag{7}$$

$$q(\boldsymbol{r}) = \frac{s(\boldsymbol{r})}{D}\ , \tag{8}$$

Eq. (5) can be written in a simple form,

$$\nabla^2\phi_s(\boldsymbol{r}) + B_m^2\phi_s(\boldsymbol{r}) + q(\boldsymbol{r}) = 0\ . \tag{9}$$

Eq. (9) is the main equation we are going to solve. We will use the Green's function method to solve this equation[9–10], where the static Green's function is defined via

$$\nabla^2 G(\boldsymbol{r}, \boldsymbol{r}') + B_m^2 G(\boldsymbol{r}, \boldsymbol{r}') + \delta(\boldsymbol{r} - \boldsymbol{r}') = 0\ , \tag{10}$$

and the neutron flux can then be obtained by

$$\phi_s(\boldsymbol{r}) = \int_V \mathrm{d}^3\boldsymbol{r}'\, G(\boldsymbol{r}, \boldsymbol{r}')q(\boldsymbol{r}')\ . \tag{11}$$

### 2.1 Cylinder case

In this subsection, we consider an infinite cylinder with radius $R$. In cylindrical coordinates, Eq. (10) is written in the following form,

$$\left[\frac{\partial^2}{\partial r^2} + \frac{1}{r}\frac{\partial}{\partial r} + \frac{1}{r^2}\frac{\partial^2}{\partial\theta^2} + B_m^2\right]G(P,P') + \delta(P,P') = 0\ , \tag{12}$$

with the boundary condition

$$G(P,P')\mid_{r=R} = 0\ . \tag{13}$$

Here we used the notation $P \equiv (r,\theta)$ and $P' \equiv (r',\theta')$.

The fundamental solution $u(r_{PP'})$ of the inhomogeneous diffusion equation satisfies

$$\begin{aligned}&\frac{\partial^2}{\partial r^2}u(r_{PP'}) + \frac{1}{r}\frac{\partial}{\partial r}u(r_{PP'}) + \frac{1}{r^2}\frac{\partial^2}{\partial\theta^2}u(r_{PP'})\\ &+B_m^2 u(r_{PP'}) = -\delta(P-P')\ ,\end{aligned} \tag{14}$$

where $r_{PP'}$ is the distance between the two points $P$ and $P'$ in the cylinder. The solution reads[11]

$$u(r_{PP'}) = -\frac{1}{4}\mathrm{Y}_0(B_m r_{PP'})\ , \tag{15}$$

where $\mathrm{Y}_0$ denotes the Bessel function of the second kind. Then the Green's function can be decomposed into two parts

$$G(P,P') = u(r_{PP'}) + g(P,P')\ , \tag{16}$$

where $g(P,P')$ is the solution of the homogeneous equation

$$\begin{aligned}&\frac{\partial^2}{\partial r^2}g(P,P') + \frac{1}{r}\frac{\partial}{\partial r}g(P,P') + \frac{1}{r^2}\frac{\partial^2}{\partial\theta^2}g(P,P')\\ &+B_m^2 g(P,P') = 0\ ,\end{aligned} \tag{17}$$

satisfying the boundary condition

$$g(P,P')\mid_{r=R} = -u(r_{PP'})\mid_{r=R}\ . \tag{18}$$

The homogeneous solution $g(P,P')$ can be expanded in the series

$$g(P,P') = \sum_{n=0}^{\infty}\mathrm{J}_n(B_m r)\Big[A_n\cos(n\theta) + B_n\sin(n\theta)\Big]\ , \tag{19}$$

where $J_n$ is the Bessel function of the first kind, $A_n$ and $B_n$ are coefficients to be determined by the boundary condition. To this end, we use trigonometric series to expand the fundamental solution at the boundary,

$$u(r_{PP'})\,|_{r=R} = -\frac{1}{4}\mathrm{Y}_0(B_\mathrm{m} r^R_{PP'}) = \sum_{n=0}^{\infty}\left[A'_n\cos(n\theta)+B'_n\sin(n\theta)\right], \tag{20}$$

where $r^R_{PP'} = \sqrt{R^2+r'^2-2Rr'\cos(\theta-\theta')}$. Then the coefficients are obtained as

$$A'_n = -\frac{1}{4\pi\omega_n}\int_0^{2\pi}\mathrm{d}\theta\,\mathrm{Y}_0(B_\mathrm{m} r^R_{PP'})\cos(n\theta),$$
$$B'_n = -\frac{1}{4\pi}\int_0^{2\pi}\mathrm{d}\theta\,\mathrm{Y}_0(B_\mathrm{m} r^R_{PP'})\sin(n\theta), \tag{21}$$

where

$$\omega_n = \begin{cases} 2, & n=0 \\ 1, & n\neq 0 \end{cases}. \tag{22}$$

At the boundary, Eq. (19) reads

$$g(P,P')\,|_{r=R} = \sum_{n=0}^{\infty}\mathrm{J}_n(B_\mathrm{m}R)\left[A_n\cos(n\theta)+B_n\sin(n\theta)\right]. \tag{23}$$

Comparing the coefficients in Eqs. (20) and (23), we obtain

$$A_n = \frac{1}{4\pi\omega_n \mathrm{J}_n(B_\mathrm{m}R)}\int_0^{2\pi}\mathrm{d}\theta\,\mathrm{Y}_0(B_\mathrm{m} r^R_{PP'})\cos(n\theta),$$
$$B_n = \frac{1}{4\pi \mathrm{J}_n(B_\mathrm{m}R)}\int_0^{2\pi}\mathrm{d}\theta\,\mathrm{Y}_0(B_\mathrm{m} r^R_{PP'})\sin(n\theta). \tag{24}$$

Finally, the series solution of the Green's function of the diffusion equation in cylindrical coordinates reads

$$G(P,P') = -\frac{1}{4}\mathrm{Y}_0(B_\mathrm{m} r_{PP'}) + \sum_{n=0}^{\infty}\mathrm{J}_n(B_\mathrm{m}r)\times \left[A_n\cos(n\theta)+B_n\sin(n\theta)\right], \tag{25}$$

when the source is at the center of the cylinder, the Green's function is reduced to a simple form,

$$G(r,0) = -\frac{1}{4}\mathrm{Y}_0(B_\mathrm{m}r) + \frac{1}{4}\frac{\mathrm{Y}_0(B_\mathrm{m}R)}{\mathrm{J}_0(B_\mathrm{m}R)}\mathrm{J}_0(B_\mathrm{m}r). \tag{26}$$

## 2.2 Sphere case

In this subsection, we consider a finite spherical subcritical core with radius $R$. Although a real reactor has rarely been designed in the shape of a sphere, it is still worth investigating as a practical three-dimensional model. In spherical coordinates, Eq. (10) becomes

$$\left[\frac{1}{r^2}\frac{\partial}{\partial r}\left(r^2\frac{\partial}{\partial r}\right)+\frac{1}{r^2}\frac{\partial^2}{\partial\theta^2}+\frac{1}{r^2\tan\theta}\frac{\partial}{\partial\theta}+\frac{1}{r^2\sin\theta}\frac{\partial^2}{\partial\varphi^2}+ B^2_\mathrm{m}\right]G(P,P')+\delta(P,P')=0, \tag{27}$$

with the boundary condition

$$G(P,P')\,|_{r=R} = 0. \tag{28}$$

Here our notation for $P$ and $P'$ becomes $P\equiv(r,\theta,\varphi)$ and $P'\equiv(r',\theta',\varphi')$.

Following the same procedure as in subsection 2.1, it is natural to obtain the series expression of the Green's function in spherical coordinates,

$$G(P,P') = -\frac{1}{4\pi}\frac{\cos(B_\mathrm{m} r_{PP'})}{r_{PP'}} + \left(\frac{r}{R}\right)^{1/2}\times \sum_{n_1=0}^{\infty}\sum_{n_2=0}^{n_1}\frac{\mathrm{J}_{n_1+1/2}(B_\mathrm{m}r)}{\mathrm{J}_{n_1+1/2}(B_\mathrm{m}R)}\times [C_{n_1n_2}F^{(1)}_{n_1n_2}(\theta,\varphi)+D_{n_1n_2}F^{(2)}_{n_1n_2}(\theta,\varphi)], \tag{29}$$

where $C_{n_1n_2}$ and $D_{n_1n_2}$ are coefficients, $F^{(1)}_{n_1n_2}$ and $F^{(2)}_{n_1n_2}$ are orthogonal functions in the series expansion of the boundary condition,

$$F^{(1)}_{n_1n_2} = \sin^{n_2}(\theta)\left[C^{1/2}_{n_1}(\cos\theta)\right]^{n_2}\cos(n_2\varphi),$$
$$F^{(2)}_{n_1n_2} = \sin^{n_2}(\theta)\left[C^{1/2}_{n_1}(\cos\theta)\right]^{n_2}\sin(n_2\varphi). \tag{30}$$

Here $C^\lambda_n$ are ultra-spherical polynomials and given by[12]:

$$C^\lambda_n(\cos\theta) = \frac{1}{\Gamma(\lambda)}\sum_{l=0}^{[n/2]}\frac{(-1)^l\Gamma(\lambda+n-l)}{l!(n-2l)!}(2\cos\theta)^{(n-2l)}. \tag{31}$$

The coefficients $C_{n_1n_2}$ and $D_{n_1n_2}$ are determined by the boundary condition,

$$C_{n_1n_2} = \frac{1}{4N^2\pi^2\omega_{n_2}}\int_0^{2\pi}\int_0^{\pi}\mathrm{d}\theta\mathrm{d}\varphi\times \frac{1}{r^R_{PP'}}\cos(B_\mathrm{m} r^R_{PP'})F^{(1)}_{n_1n_2}(\theta,\varphi)\sin\theta,$$
$$D_{n_1n_2} = \frac{1}{4N^2\pi^2}\int_0^{2\pi}\int_0^{\pi}\mathrm{d}\theta\mathrm{d}\varphi\times \frac{1}{r^R_{PP'}}\cos(B_\mathrm{m} r^R_{PP'})F^{(2)}_{n_1n_2}(\theta,\varphi)\sin\theta, \tag{32}$$

where

$$N^2 = \frac{(n_1+n_2)!}{(n_1-n_2)!}\frac{2}{(2n_1+1)}, \tag{33}$$

$$r^R_{PP'} = \sqrt{R^2+r'^2-2Rr'\cos(\Theta)}, \tag{34}$$

with cos(Θ) defined by

$$\cos(\Theta) = \cos\theta\cos\theta' + \sin\theta\sin\theta'\cos(\varphi-\varphi') \,. \quad (35)$$

When the source is at the center of the sphere, Eq. (29) is reduced to a simple form,

$$G(r,0) = -\frac{\cos(B_m r)}{4\pi r} + \frac{\cos(B_m R)}{4\pi R}\left(\frac{r}{R}\right)^{-1/2}\frac{J_{1/2}(B_m r)}{J_{1/2}(B_m R)} \,. \quad (36)$$

Obviously the above solution satisfies the boundary condition $G(R,0)=0$.

## 2.3 Neutron flux distribution

As an example, we will numerically calculate the flux distribution of neutrons of 0.1 MeV diffusing in a multiplying material of enriched uranium dioxide in a cylinder. Firstly, we need to know the material buckling $B_m$ and the core radius $R$ in order to evaluate the Green's functions in Eqs. (26 ~ 27).

The data in Table 1 are used to calculate $B_m$ by Eq. (7). The core radius is derived via the geometric buckling which can be read from the eigenvalue equation[14]

**Table 1 Parameters of fuel materials[13]**

| Isotopes | $\sigma_s$/b | $\sigma_a$/b | $\sigma_f$/b | $\nu$ | $\rho$/(g/cm$^3$) |
|---|---|---|---|---|---|
| $^{235}$U | 9.94 | 2.01 | 1.58 | 2.44 | |
| $^{238}$U | 11.88 | 0.18 | 0 | 0 | 10.4 |
| $^{16}$O | 3.65 | $3.19\times10^{-5}$ | 0 | 0 | |

$$\hat{L}\phi(\boldsymbol{r}) = \frac{\hat{P}}{k_{eff}}\phi(\boldsymbol{r}) \,, \quad (37)$$

where $\hat{L}$ and $\hat{P}$ are destruction and production operators respectively,

$$\hat{L} = -D\nabla^2 + \Sigma_a \,, \quad (38)$$

$$\hat{P} = \nu\Sigma_f \,. \quad (39)$$

Thus Eq. (37) can be cast into the following form

$$\nabla^2\phi(\boldsymbol{r}) + B_g^2\phi(\boldsymbol{r}) = 0 \,, \quad (40)$$

where $B_g^2$ is called the geometric buckling and given by

$$B_g^2 = \frac{1}{D}\left(\frac{\nu\Sigma_f}{k_{eff}} - \Sigma_a\right) . \quad (41)$$

Then the core radius can be solved from the zero flux boundary condition. For cylindrical symmetry it is

$$R_c = \frac{2.405}{B_g} \,, \quad (42)$$

and for spherical symmetry it is

$$R_s = \frac{\pi}{B_g} \,. \quad (43)$$

Thus we have obtained the core radius as a function of subcriticality and macroscopic cross-sections.

We see that the neutron flux distribution depends on the depth of the subcritical state. For simplicity, we assume that a point source is located at the center of the core. The neutron flux can then be obtained from the Green's function in Eq. (26). As shown in Table 2 and Fig. 1, the closer the system is to the critical state, the higher the neutron flux generated per source neutron will be, implying that the less important role the external neutron source will play. In addition, as $k_{eff}$ goes to unity, the neutron flux profile will approach the shape of the Bessel function of the first kind as in the critical case. Note that we have re-scaled the neutron flux in the critical case so that it can be compared to those in subcritical ones since the neutron flux in a critical system can have arbitrary value.

**Table 2 Parameters chosen for Fig. 1**

| Status | $k_{eff}$ | $\varepsilon$ | $B_m$/m$^{-1}$ |
|---|---|---|---|
| case 1 | 0.85 | 0.0931 | 1.8094 |
| case 2 | 0.90 | 0.1032 | 3.1003 |
| case 3 | 0.95 | 0.1133 | 3.9922 |
| case 4 | 0.99 | 0.1223 | 4.4637 |

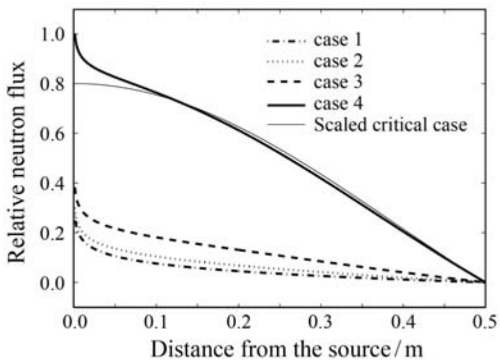


Fig. 1 Neutron flux distribution in subcritical states

Another factor that will influence the neutron flux distribution is the core size (i.e. the radius $R$ in our case). In the subcritical system, the external neutron source introduces more dependence of the neutron flux distribution on intrinsic properties of the core. The subcritical system can maintain a certain subcritical state (e.g. $k_{eff}=0.96$) by changing both the fissile material enrichment $\varepsilon$ of $^{235}$U and the radius of the core. A smaller radius corresponds to a higher enrichment. Different groups of $R$ and the corresponding $\varepsilon$ lead to different neutron flux profiles, as shown in Table 3 and Fig. 2. For larger size of the core and lower enrichment, e.g. case 1, the singularity of the flux distribution introduced by the source term is more apparent than the opposite case, e.g. case 4. We now study the impact of the external source position. Fig. 3 shows the relative neutron flux distribution (normalized by the maximal value of the neutron flux in case of Fig. 3(a) with the source at the center). $k_{\rm eff}$ is set to 0.96. The radius of the core is set to 0.8 m, and the corresponding $\varepsilon$ is solved to be 0.094 7. The source position is denoted by $r'$. The maximum value of the neutron flux always appears at the source position. As the source moves to the boundary off the center, the neutron flux becomes lower due to higher neutron escape probability near the boundary.

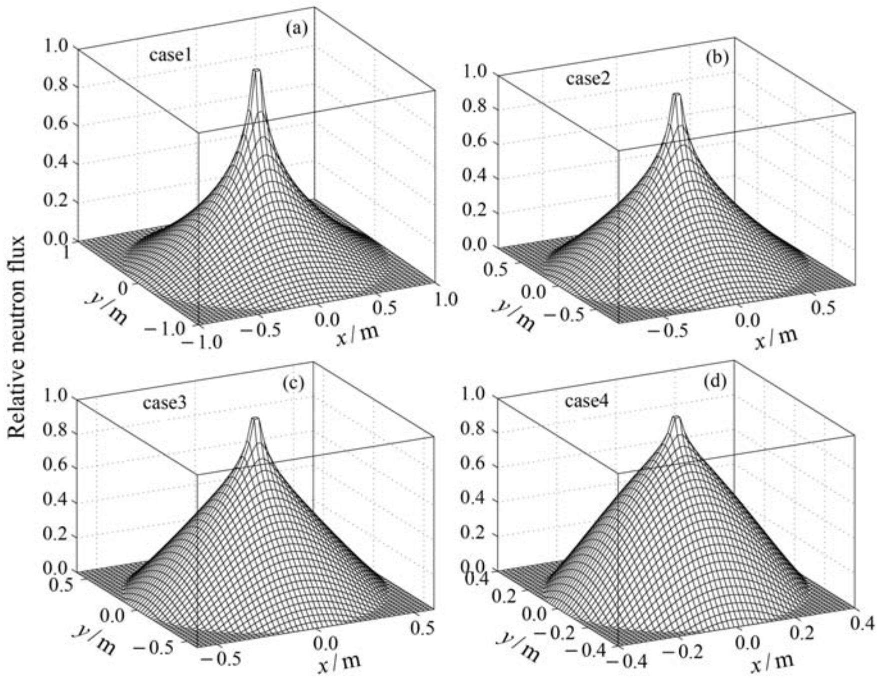


Fig. 2　(color online) Relative neutron flux distribution in a certain subcritical state when the source position is at the center.

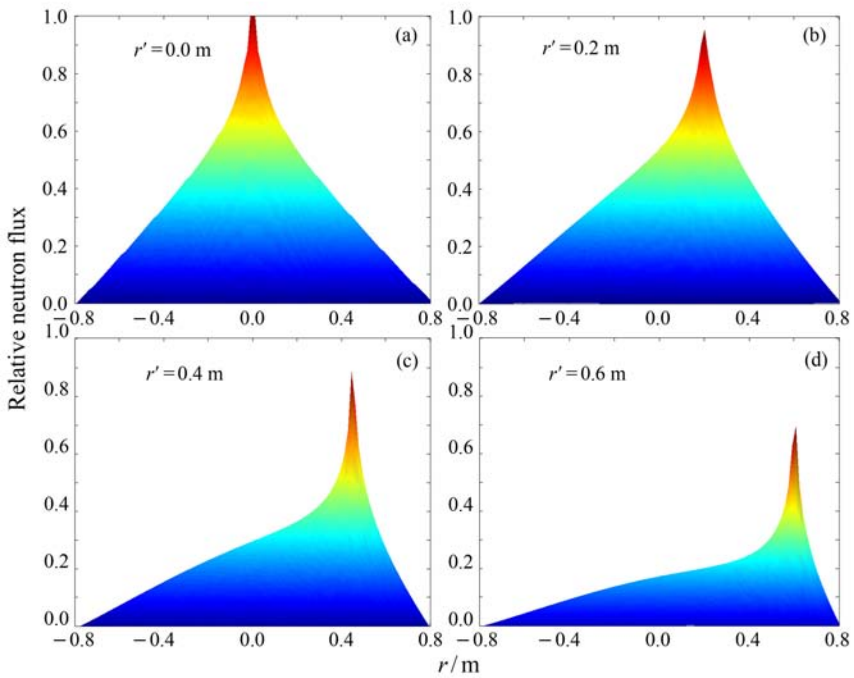


Fig. 3　(color online) Relative neutron flux distributions in a certain subcritical state with source positions at or off the center.

**Table 3 Parameters in the one group cylindrical model**

| Status | $R$/m | $\Sigma_s$/m$^{-1}$ | $\Sigma_a$/m$^{-1}$ | $\Sigma_f$ /m$^{-1}$ | $B_m$/m$^{-1}$ | $B_g$/m$^{-1}$ | $\varepsilon$ |
|---|---|---|---|---|---|---|---|
| case 1 | 1 | 44.110 3 | 0.804 3 | 0.333 5 | 1.124 1 | 2.3981 | 0.0899 |
| case 2 | 0.8 | 44.090 9 | 0.824 9 | 0.351 3 | 2.068 5 | 3.000 6 | 0.094 7 |
| case 3 | 0.6 | 43.048 7 | 0.869 6 | 0.389 9 | 3.286 7 | 4.005 1 | 0.105 1 |
| case 4 | 0.4 | 43.928 7 | 0.996 9 | 0.499 7 | 5.413 0 | 5.999 6 | 0.134 7 |

# 3 Subcritical multiplication factor

We know from Eqs. (1 ~ 4) that the subcritical multiplication factor $k_s$ is related to the neutron flux. In the previous section, we have analyzed how the core properties and the external source influence the neutron flux distribution. In this section we will calculate $k_s$ and study its dependence on the core properties and the external source. We will show how the values of $k_s$ and $k_{eff}$ depend on the core radius $R$, the corresponding fissile material enrichment $\varepsilon$ and the source position $r'$.

We also consider the cylinder case as an example. When the source is at the center of the core, the integrated neutron flux becomes (see Appendix A for detailed derivation)

$$\int_V d^3\boldsymbol{r}\,\phi_s(\boldsymbol{r}) = 2\pi\int_V dr\,G(r,0)r = -\frac{\pi R}{2B_m}\left[Y_1(B_mR)+\frac{2}{B_mR\pi}-\frac{Y_0(B_mR)}{J_0(B_mR)}J_1(B_mR)\right]. \quad (44)$$

Thus total numbers of fission neutrons $F$ and source neutrons $S$ are given by

$$F = \nu\Sigma_f\int_V d^3\boldsymbol{r}\phi_s(\boldsymbol{r}) = -\frac{\nu\Sigma_f\pi R}{2B_m}\times\left[Y_1(B_mR)+\frac{2}{B_mR\pi}-\frac{Y_0(B_mR)}{J_0(B_mR)}J_1(B_mR)\right],$$
$$S = \int_V d^3\boldsymbol{r}s(\boldsymbol{r}) = \int_V d^3\boldsymbol{r}D\delta(\boldsymbol{r}) = D. \quad (45)$$

Then $k_s$ can be calculated from Eqs. (144 ~ 45). As pointed out in section 2, in order to maintain a certain subcritical state, we need to modify both the fissile material enrichment and the core size for a balance between the fission reaction rate and the neutron leakage. This is the same as in a critical state. However, the source driven subcritical system has more complicated neutron balance relation. Since external source neutrons are not generated by the core's fission reaction, the effects of changing the enrichment and the core radius are different for fission neutrons from source neutrons. For instance, we increase the core size and correspondingly decrease the enrichment, then the fission reaction rate will decrease. Since the source neutrons mainly come from the center and are less sensitive to the increasing leakage effect than average fission neutrons. This means larger proportion of leakage neutrons in the total fission neutrons than for external source neutrons. According to Eqs. (1 ~ 4), $k_s$ will decrease with the core radius.

The results for $k_s$ as a function of $R$ are shown in Fig. 4. The corresponding fissile material enrichment ranges from 0.09 to 0.13 for each subcriticality $k_{eff}$. We see that $k_s$ slightly decreases with the core radius, which is consistent to the above arguments. Although the decrease is small, it is still expected to have an impact on the energy gain, because it is proportional to $k_s/(1-k_s)$ as in Eq. (4) and $k_s$ is normally set to values close to unity by design in practical subcritical reactors. We also see that $k_s$ is always larger than $k_{eff}$ when the source is placed at the center of the core due to a high source neutron efficiency. And the difference between $k_s$ and $k_{eff}$ will be smaller as they approach unity.

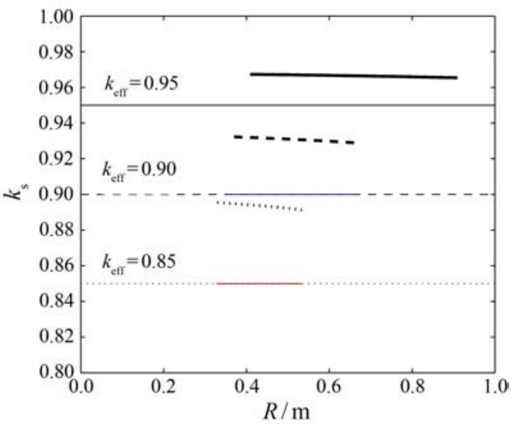


Fig. 4 (color online) $k_s$ as a function of the core radius.

Shown in Fig. 5 is the multiplication factor $k_s$ as a function of the external source position $r'$. We set $k_{eff}$ = 0.95 and $R$ = 0.5 m. When the source is off the center, the expression for the Green's function for the neutron flux is complicated as shown in Eq. (25). It is impossible to obtain an analytical form of the neutron flux from Eq. (25). So we choose five different source positions ($r'$=0, 0.1, 0.2, 0.3 and 0.4 m) and numerically calculate the integral of the neutron flux to give $k_s$. The results indicate that the highest value of $k_s$ is achieved when the source is at the center and source neutrons have the largest multiplication efficiency. As the source moves to the boundary, the leakage effect will play a more important role on source neutrons, thus $k_s$ becomes smaller. When the source is at a certain distance from the center, the difference between $k_s$ and $k_{eff}$ will disappear, which means source neutrons have the same multiplication capability as the average fission neutrons.

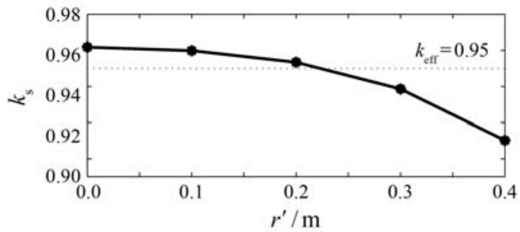


Fig. 5　$k_s$ as a function of the source position

# 4 Conclusion

We apply the Fourier method to obtain Green's functions of the one group inhomogeneous neutron diffusion equation in cylindrical and spherical symmetries. Based on these analytical solutions, we have studied the dependence of the neutron flux on the subcriticality, the size of the subcritical system and the position of the external neutron source.

For most of source positions, $k_s$ is different from $k_{eff}$. Thus, using the conventional subcriticality $k_{eff}$ to evaluate the neutron production capability will lead to considerable inaccuracy. For certain subcritical states, $k_s$ varies with the core size. Although this variation is small, the energy gain is sensitive to $k_s$ and then the core size, which has to be taken into account in the design of the source driven subcritical system.

# 5 Appendix

## 5.1 Some discussions on the singularity of the neutron flux distribution at source position

The external source term will lead to divergence in the neutron flux at the source position, see Eqs. (26 ~ 27). It is due to the invalidity of the diffusion approximation from the Fick's law at or very close to the source position. Thus, for analysis purpose, we use the neutron flux at 2 cm off the source position as the maximum value in plotting the neutron flux profiles.

However, the integral of the neutron flux is finite and makes the subcritical multiplication factor $k_s$ regular. To obtain Eq. (44), we need to prove the convergence of $\int_0^R \mathrm{d}r\, \mathrm{Y}_0(B_\mathrm{m} r) r$, which can be written as

$$\int_0^R \mathrm{d}r\, \mathrm{Y}_0(B_\mathrm{m} r) r = \frac{1}{B_\mathrm{m}^2}\left[\mathrm{Y}_1(B_\mathrm{m}R)B_\mathrm{m}R - \epsilon \mathrm{Y}_1(\epsilon)\,|_{\epsilon\to 0}\right]. \quad (46)$$

The Bessel function of the first kind has the series form[12],

$$\mathrm{J}_{\pm\nu}(z) = \sum_{k=0}^{\infty} \frac{(-1)^k}{k!}\frac{1}{\Gamma(\pm\nu+k+1)}\left(\frac{z}{2}\right)^{(2k\pm\nu)}. \quad (47)$$

From

$$\mathrm{Y}_n(z) = \frac{1}{\pi}\left\{\frac{\partial \mathrm{J}_\nu}{\partial \nu} - (-1)^n \frac{\partial \mathrm{J}_{-\nu}}{\partial \nu}\right\}_{\nu\to n}, \quad (48)$$

the Bessel function of the second kind becomes

$$\mathrm{Y}_n(z) = \frac{2}{\pi}\mathrm{J}_n(z)\ln\frac{z}{2} - \frac{1}{\pi}\sum_{k=0}^{n-1}\frac{(n-k-1)!}{k!}\left(\frac{z}{2}\right)^{(2k-n)} - \frac{1}{\pi}\sum_{k=0}^{\infty}\frac{(-1)^k}{k!(n+k)!}\Big[\psi(n+k+1)+ \psi(k+1)\Big]\left(\frac{z}{2}\right)^{(2k+n)}. \quad (49)$$

where $\psi(z) = \Gamma'(z)/\Gamma(z)$ and $\Gamma(z)$ is the Gamma function. When $n \geqslant 1$ and $z \to 0$, the first and third terms of Eq. (49) go toward zero, left with only the second term,

$$\mathrm{Y}_n(z) \sim \frac{(n-1)!}{\pi}\left(\frac{z}{2}\right)^{(-n)}, \quad (n \geqslant 1), \quad (50)$$

and so we have $\lim_{z\to 0} z\mathrm{Y}_1(z) = 2/\pi$.

**References:**

[1] CARMINATI F, KLAPISCH R, REVOL J P, *et al*. CERN/AT/93-47(ET), 1993.

[2] RUBBIA C, RUBIO J A, BUONO S, *et al*. CERN/AT/95-44(ET), 1995.

[3] GANDINI A, SALVATORES M. Journal of Nuclear Science and Technology, 2002, **39**(6): 673.

[4] SHAHBUNDER H, PYEON C H, MISAWA T, *et al*. Annals of Nuclear Energy , 2010, **37**: 592.

[5] SHAHBUNDER H, PYEON C H, MISAWA T, *et al*. Annals of Nuclear Energy , 2010, **37**: 1214.

[6] SHAHBUNDER H, PYEON C H, MISAWA T, *et al*. Annals of Nuclear Energy, 2010, **37**: 1785.

[7] NIFENECKER H, DAVID S, LOSISEAUX M J, *et al*. Nuclear Instruments and Methods in Phyiscs Research A, 2001, **463**: 428.

[8] SHI Yongqian, ZHU Qingfu, TAO He, *et al*. Nuclear Technology, 2005, **149**(1): 122.

[9] WRIGHT J, PAZSIT I. Annals of Nuclear Energy, 2006, **33**: 149.

[10] KOBAYASHI K, NISHIHARA K. Nuclear Science and Engineering, 2000, **136**: 272.

[11] YAN Zhenjun. Mathematical Physical Equation [M]. Second edition. Hefei: University of Science and Technology of China Press, 2010: 197–201. (in Chinese)
(严镇军. 数学物理方程 [M]. 第二版. 合肥: 中国科技大学出版社, 2010: 197-201.)

[12] WANG Zhuxi GUO Dunren. Introduction to Special Function [M]. Beijing: Peking University Press, 2000: 268-271, 355-358 (In Chinese).
(王竹溪, 郭敦仁. 特殊函数概论 [M]. 北京: 北京大学出版社, 2000: 268–271, 355–358.)

[13] YOUNG, CHADWICK, TALOU. ENDF/B-VII.1 (USA2011). [EB/OL]. [2013-03-10]. http://www-nds.iaea.org/exfor/endf.htm.

[14] BELL G, GLASSTONE S. Nuclear Reactor Theory [M]. New York: Van Nostrand Reinhold Company, 1970: 39–48.

# 加速器驱动次临界系统中非齐次中子扩散方程的一种解析解

井 田[1]，王相綦[1]，王 群[2]，武红利[1]，龚晓冬[1]

(1. 中国科技大学国家同步辐射实验室，安徽 合肥 230029；
2. 中国科技大学近代物理系，安徽 合肥 230027)

**摘要：** 利用傅里叶方法得到了非齐次中子扩散方程格林函数的解析形式，通过格林函数计算了当外源在堆芯任意位置时的中子通量密度分布，分析了在次临界反应堆系统中，次临界倍增系数 $k_s$ 与外源位置和相同次临界深度下堆芯尺寸的依赖关系。发现，$k_s$ 随着堆芯尺寸的增加而减小，这点变化虽小，但能量增益对 $k_s$ 以及堆芯尺寸是相当敏感的，加速器驱动的次临界系统 (ADS) 设计时应必须予以考虑。

**关键词：** ADS；中子通量密度；中子扩散方程；次临界倍增系数；次临界度

---

**收稿日期：** 2013-04-15； **修改日期：** 2013-05-04

**基金项目：** 国家自然科学基金资助项目(11045003，10975150)

**通信作者：** 王相綦，E-mail: wangxaqi@ustc.edu.cn; 王群，E-mail: qunwang@ustc.edu.cn